A Control Technique for Integration of DG Units to the Electrical Networks

Edris Pouresmaeil, Carlos Miguel-Espinar, Miquel Massot-Campos, Daniel Montesinos-Miracle, *Member, IEEE*, and Oriol Gomis-Bellmunt, *Senior Member, IEEE*

***Abstract*—This paper deals with a multiobjective control technique for integration of distributed generation (DG) resources to the electrical power network. The proposed strategy provides compensation for active, reactive, and harmonic load current components during connection of DG link to the grid. The dynamic model of the proposed system is first elaborated in the stationary reference frame and then transformed into the synchronous orthogonal reference frame. The transformed variables are used in control of the voltage source converter as the heart of the interfacing system between DG resources and utility grid. By setting an appropriate compensation current references from the sensed load currents in control circuit loop of DG, the active, reactive, and harmonic load current components will be compensated with fast dynamic response, thereby achieving sinusoidal grid currents in phase with load voltages, while required power of the load is more than the maximum injected power of the DG to the grid. In addition, the proposed control method of this paper does not need a phase-locked loop in control circuit and has fast dynamic response in providing active and reactive power components of the grid-connected loads. The effectiveness of the proposed control technique in DG application is demonstrated with injection of maximum available power from the DG to the grid, increased power factor of the utility grid, and reduced total harmonic distortion of grid current through simulation and experimental results under steady-state and dynamic operating conditions.**

Manuscript received January 27, 2012; revised April 16, 2012 and June 11, 2012; accepted June 28, 2012. Date of publication July 19, 2012; date of current version February 28, 2013.

E. Pouresmaeil was with the Centre d'Innovació Tecnològica en Convertidors Estàtics i Accionaments (CITCEA-UPC), Departament d'Enginyeria Elèctrica, and Escola Tecnica Superior d'Enginyeria Industrial de Barcelona, Universitat Politècnica de Catalunya, 08028 Barcelona, Spain. He is now with the Department of Electrical and Computer Engineering, University of Waterloo, Waterloo, ON N2L-3G1 Canada (e-mail: edris.pouresmaeil@uwaterloo.ca).

C. Miguel-Espinar and D. Montesinos-Miracle are with the Centre d'Innovació Tecnològica en Convertidors Estàtics i Accionaments (CITCEA-UPC), Departament d'Enginyeria Elèctrica, and Escola Tecnica Superior d'Enginyeria Industrial de Barcelona, Universitat Politècnica de Catalunya, 08028 Barcelona, Spain (e-mail: carlos.miguel@citcea.upc.edu; montesinos@citcea.upc.edu).

M. Massot-Campos was with the Centre d'Innovació Tecnològica en Convertidors Estàtics i Accionaments (CITCEA-UPC), Universitat Politècnica de Catalunya, 08028 Barcelona, Spain. He is now with the Systems, Robotics and Vision Group, Departament de Matematiques i Informatica, Universitat de les Illes Balears, 07122 Palma de Mallorca, Spain (e-mail: miquel.massot@uib.cat).

O. Gomis-Bellmunt is with the Centre d'Innovació Tecnològica en Convertidors Estàtics i Accionaments (CITCEA-UPC), Departament d'Enginyeria Elèctrica, and Escola Tecnica Superior d'Enginyeria Industrial de Barcelona, Universitat Politècnica de Catalunya, 08028 Barcelona, Spain, and also with the Catalonia Institute for Energy Research (IREC), 08930 Barcelona, Spain (e-mail: gomis@citcea.upc.edu).

Color versions of one or more of the figures in this paper are available online at http://ieeexplore.ieee.org.

Digital Object Identifier 10.1109/TIE.2012.2209616

***Index Terms*—Digital signal processor, distributed generation (DG), renewable energy sources, total harmonic distortion (THD), voltage source converter (VSC).**

I. Introduction

DISTRIBUTED generation (DG) technology also known as dispersed generation technology is electricity generating plant connected to a distribution grid rather than the transmission network. There are many types and sizes of DG facilities. These include wind farms, solar photovoltaic (PV) systems, hydroelectric power, or one of the new smaller generation technologies. The DG concept emerged as a way to integrate different power plants, increasing the DG owner's reliability and security, providing additional power quality benefits of the power grid [1], [2], and improving the air quality as a result of lower greenhouse gas emissions of air pollutants [3], [4]. In addition, the cost of the distribution power generation system using the renewable energies is on a falling trend and is expected to fall further as demand and production increase [5].

DG technology can come from conventional technologies such as motors powered by natural gas or diesel fuel or from renewable energy technologies, such as solar PV cells and wind farms.

Over the past two decades, declines in the costs of small-scale electricity generation, increases in the reliability needs of many customers, and the partial deregulation of electricity markets have made DG technology more attractive to businesses and households as a supplement to utility-supplied power [6]. However, the increasing number of DG units in electrical networks requires new techniques for the operation and management of the power networks in order to maintain or even to improve the power supply reliability and quality in the future. As a consequence, the control of DG unit should be improved to meet the requirements for the electrical network. Therefore, design of a control technique, which considers different situations of the electrical networks, becomes of high interest for interconnection of DG units to the power grid.

Numerous control techniques and strategies have been proposed and reported for the control and connection of DG units to the electrical grid [7]. In [8], an overview of different control and synchronization techniques for DG systems has been presented. Different hardware structures for the DG system [9], control strategies for the grid-side converter, and control strategies under fault conditions were addressed [10], [11]. Different implementation techniques like dq, stationary, and natural frame control structures were presented, and their major characteristics were pointed out [12]. A discussion about

different controllers in DG system and their ability to compensate low-order harmonic components presented in the utility grid was given [13]. Finally, an overview of grid synchronization strategies, their influences, and roles in the control of DG system on normal and faulty grid conditions were discussed [14]. In [15], a control concept was proposed that provides sharing of harmonic load currents between parallel-connected converters without mutual communication. In this paper, a converter operates as an active inductor at a certain frequency to absorb the harmonic current components. However, the exact calculation of grid inductance in real-time systems is not simple, and it can deteriorate the performance of the proposed control strategy. The fact that power grids are faced with unexpected and unavoidable disturbances and uncertainties complicates the design of a practical plug-and-play converter-based DG interface. A robust interfacing scheme for DG converters featuring robust mitigation of converter grid resonance at parameter variation, grid-induced distortion, and current-control parametric instabilities is presented in [16]. To ensure high disturbance rejection of grid distortion, converter resonance at parameter variation, and parametric instabilities, an adaptive internal model for the capacitor voltage and grid-side current dynamics is included within the current-feedback structure. In [17], a control algorithm of three-phase voltage source converter (VSC) has been proposed for integration of renewable energy resources to the main grid through an output L-type or LCL-type filter. The proposed controller provides active damping of the LCL resonance mode, robustness with respect to grid frequency, and impedance uncertainty. A control technique is proposed in [18], to determine which power lines should be inserted into the power network to optimize voltage profile during the presence of DG. In [19], an algorithm is suggested in order to design feasible line drop compensation parameters. This algorithm guarantees the satisfaction of voltage constraints for all possible variations in DG output. In [20], DG unit was modeled as a PV node, and its control was coordinated with existing volt/var controls to minimize distribution losses. In [21], a centralized control algorithm is proposed to operate the control devices using a communication. The proposed control technique aims that active control of DG output and volt/var regulators be in desirable level in order to allow for higher levels of distributed resource integrations. A loss reduction and approximate power flow formula were suggested in [22] and [23] to aid the search for optimal feeder configuration for loss minimization. The impact of DG technology on distribution feeder reconfiguration was described in [24]. In this paper, the cost summation of electrical power generated by DG technology and from substation buses was analyzed.

Several other control strategies of interfacing system between DG resources and electrical grid proposed and presented for different objectives [1], [25]–[28]. In all the proposed methods, a solution has been proposed for an important problem in electrical networks. In this paper, the authors propose a design of a multipurpose control strategy for VSC used in DG system. The idea is to integrate the DG resources to the power grid. With the proposed approach, the proposed VSC controls the injected active power flow from the DG source to the grid and also performs the compensation of reactive power and the nonlinear load current harmonics, keeping the grid current almost sinusoidal during connection of extra loads to the grid.

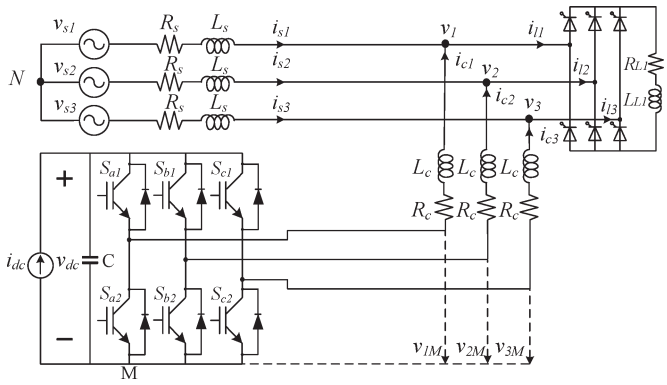

Fig. 1. Schematic diagram of the proposed DG system.

The exact feedback linearization theory is applied in the design of the proposed controller. This control technique allows the decoupling of the currents and enhances their tracking of the fast change in the active and reactive power.

This paper shows the complete simulation and experimental validation of the proposed method for all its features, i.e., active and reactive power generation along with current harmonic compensation.

This paper is organized as follows. The proposed system's model is introduced and discussed in detail in Section II, with a particular focus on the reference current generator. Sections III and IV are related to the modeling of the proposed DG system, with focus on the dynamic and state-space model analysis for control and the current control implementation.

Simulation results of the proposed system are presented in Section V for different conditions. Section VI is related to the experimental results and contains a description of the testing setup followed by a complete experimental validation of the proposed control technique. The experimental results are presented for the grid-connected VSC that generates maximum active power of DG source and compensates for unwanted reactive and harmonic load current component nonlinear loads, thus achieving complete power quality features.

II. Proposed DG Model

Fig. 1 shows the schematic diagram of the proposed system. Conventional signs of voltages and currents components are also indicated in this schema, where R_c and L_c represent the equivalent resistance and inductance of the ac filter, coupling transformer, and connection cables; R_s and L_s represent the grid resistance and inductance up to the point of common coupling (PCC), respectively; v_k ($k = 1, 2, 3$) is the supply voltage components at the PCC; v_{sk} is the grid voltage components; $v_{\rm dc}$ is the dc-link voltage; and i_{sk}, i_{lk}, and i_{ck} are grid, load, and DG current components, respectively. In addition, the DG resources and additional components are represented as a dc current source which is connected to the dc side of the converter.

III. Voltage and Current Components in the Special Reference Frames

The proposed control technique in this paper is based on the analysis of voltage and current vector components in the

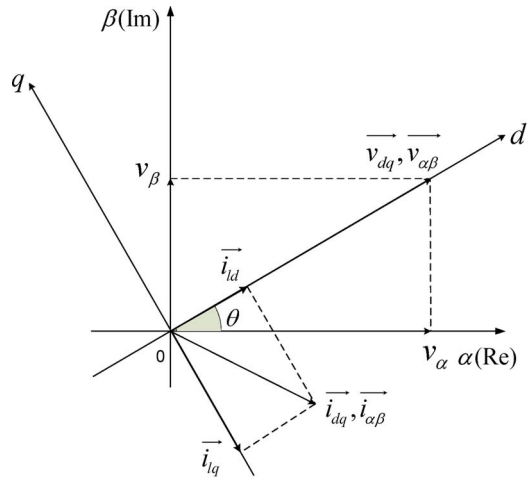

Fig. 2. Voltage and current components in special reference frames.

special reference frames, e.g., 123(abc) to $\alpha\beta$ and $\alpha\beta$ to dq transformation. The Clarke transformation maps the three-phase instantaneous voltages and currents in the 123 phases into the instantaneous voltages and currents on the $\alpha\beta$-axes. In the next step, the $\alpha\beta$ reference frame is transformed to the rotating synchronous reference frame, i.e., in dq-components. The synchronous reference frame uses a reference frame transformation module, to transform the grid current and voltage waveforms into a reference frame that rotates synchronously with the grid voltage. By means of this, the control variables become dc values; thus, filtering and controlling can be achieved easily [29].

Fig. 2 shows the voltage and current components in $\alpha\beta$ and dq reference frames. Considering d-axis vector in the direction of voltage vector in this transformation, the q-component of voltage in rotating synchronous reference frame is always zero $(v_q = 0)$ [30]. Therefore, the instantaneous angle of grid voltage can be calculated as

$$\theta = \tan^{-1}\frac{v_\beta}{v_\alpha}. \tag{1}$$

In other words, if we consider the instantaneous angle of load voltage by (1), the reference voltage vector will be in the direction of d-axis vector of load voltage, and q-axis vector of load voltage will be zero.

According to Fig. 2, the magnitude of the voltage at the PCC can be calculated as

$$v_{\rm ref} = |\overrightarrow{v_d}| = |\overrightarrow{v_{dq}}| = |\overrightarrow{v_{\alpha\beta}}| = \sqrt{v_\alpha^2 + v_\beta^2}. \tag{2}$$

In the next stage, reference currents of the DG control loop must be calculated according to the objectives of the proposed DG model.

A. Calculation of Reference Current to Supply Load Active Power

In fundamental frequency, the active power injected from DG link to the grid is

$$P = \frac{3}{2}(v_d I_{cd} + v_q I_{cq}) \tag{3}$$

where capital letters are related to fundamental frequency of the currents. Therefore, by considering the first assumption $(v_q = 0)$, d-component of reference current to provide active current in fundamental frequency can be calculated by

$$I_{cd}^* = \frac{2}{3}\frac{P_{\rm ref}}{v_d} \tag{4}$$

where $P_{\rm ref}$ is maximum power of the VSC in fundamental frequency and I_{cd}^* is the d-component of DG link reference current in fundamental frequency. Due to limited output power of proposed VSC, reference current must be restricted. Calculation of d-component of reference current with this method makes it possible to control the maximum active power injection into the grid by changing $P_{\rm ref}$. $P_{\rm ref}$ depends on DG system capacity, capacity of power electronic interfacing devices and transformers.

B. Calculation of Harmonic Components of d-Axis Reference Current

In the dq reference frame, the fundamental current component can be seen as a dc component, and as a consequence, the harmonic load currents can be extracted with high-pass filters (HPFs). The main problem with this method is the delay that occurs when the control system is digitally implemented. To minimize the influence of the HPF phase responses, by means of a low-pass filter (LPF), a minimal phase HPF (MPHPF) can be obtained, and the transfer function of this LPF has order and cutoff frequency as the same as HPF. Thus, the MPHPF can be obtained simply by the difference between the input signal and the filtered one, which is equivalent to performing $H_{\rm MPHPF}(s) = 1 - H_{\rm LPF}(s)$. A double-precision filter using the Chebyshev type-II fifth-order LPF is used for this purpose. The filter considered has a cutoff frequency $f_c = (f/2)(f = 50$ Hz) which promises the extraction of dc components in the nonlinear load currents [31]. Therefore, i_{ld} can be expressed as

$$i_{ld} = \tilde{i_{ld}} + I_{ld} \tag{5}$$

where $\tilde{i_{ld}}$ is alternative d-component of load current which is related to harmonic components of load current and I_{ld} is the dc term of load current which is related to fundamental frequency of load current [7]. To use DG link as an active power filter, harmonic components of the nonlinear load current must be supplied. For this purpose, d-component of nonlinear link reference current is achieved by doing the sum of currents in (4) and alternative terms of load current in (5)

$$i_{cd}^* = \tilde{i_{ld}} + \overset{*}{I}\, cd. \tag{6}$$

C. Calculation of Reference Current to Supply Load Reactive Power

In dq frame, quadrature component of load current is perpendicular to direct component of voltage $(v_d \perp i_{lq})$. As a result, q-component of load current indicates required reactive power of the load. To compensate load reactive power, DG must provide a current with q-component equal to i_{lq}. For this purpose, it

is sufficient to set q-component of DG's reference current equal to q-component of the load current as

$$i^*_{cq} = i_{lq}. \tag{7}$$

The term of i^*_{cq} is the q-component of DG link reference current. By this consideration, total load reactive current and harmonic components of q-axis are compensated [32].

IV. Modeling of the Proposed DG System

For the purposes of this paper, the electric power grid is composed of the generation system, the transmission, or the distribution system, and the loads. The DG source and additional components are represented as a dc current source connected to the dc side of the proposed converter. To draw an appropriate plan to control the integration of DG resources to the power grid, a dynamic analytical model of the proposed power system should be developed.

A. Proposed Model Analysis

Kirchhoff's laws of voltage and current applied to the proposed model shown in Fig. 1 provide a general equation in the stationary reference frame in a three-phase system as

$$\sum_{i=1}^{3} v_{iM} = \sum_{i=1}^{3} \left(L_c \frac{di_{ci}}{dt} + R_c i_{ci} + v_i + v_{NM} \right). \tag{8}$$

A null value for the zero voltage component is assumed. Since the absence of neutral wire is considered, the zero current component is also null, with the assumption that the grid voltages are balanced. By taking into account these assumptions, the ac neutral point voltage term can be obtained as

$$v_{NM} = \frac{(v_{1M} + v_{2M} + v_{3M})}{3} = \frac{1}{3} \sum_{i=1}^{3} v_{iM}. \tag{9}$$

The switching function s_k of the kth leg of the VSC can be expressed as

$$S_k = \begin{cases} 1, & \text{if } T_k \text{ is on and } T'_k \text{ is off} \\ 0, & \text{if } T_k \text{ is off and } T'_k \text{ is on.} \end{cases} \tag{10}$$

Thus, with $v_{kM} = S_k v_{\mathrm{dc}}$ and substituting in (8) and (9), a set of dynamic equations describing the switched model of the proposed DG model is developed. This model is general, complete, and makes no assumptions other than the use of ideal switches. Therefore, (11) can be expressed as

$$\frac{di_{ck}}{dt} = -\frac{R_c}{L_c} i_{ck} + \frac{1}{L_c} \left(S_k - \frac{1}{3} \sum_{j=1}^{3} S_j \right) v_{\mathrm{dc}} - \frac{v_k}{L_c} \qquad k = 1, 2, 3. \tag{11}$$

Equation (11) represents phase k dynamic equation of the proposed VSC. By (11), the switching state function can be defined as

$$D_{nk} = \left(S_k - \frac{1}{3} \sum_{j=1}^{3} S_j \right). \tag{12}$$

Equation (12) shows that the value of D_{nk} depends on the switching state n and on the phase k. In other words, D_{nk} depends simultaneously on the switching functions of the three legs of the interfaced VSC. This shows the interaction between the three phases.

By substituting (12) into (11), dynamic equation of the proposed model can be expressed as

$$\frac{d}{dt} \begin{bmatrix} i_{c1} \\ i_{c2} \\ i_{c3} \end{bmatrix} = -\frac{R_c}{L_c} \begin{bmatrix} 1 & 0 & 0 \\ 0 & 1 & 0 \\ 0 & 0 & 1 \end{bmatrix} \begin{bmatrix} i_{c1} \\ i_{c2} \\ i_{c3} \end{bmatrix} + \frac{1}{L_c} \begin{bmatrix} D_{n1} \\ D_{n2} \\ D_{n3} \end{bmatrix} v_{\mathrm{dc}} - \frac{1}{L_c} \begin{bmatrix} v_1 \\ v_2 \\ v_3 \end{bmatrix}. \tag{13}$$

V. State-Space Model of Proposed System

By use of Park transformation matrix, the dynamic equations of proposed model can be transformed to the dq frame as

$$\frac{d}{dt} \begin{bmatrix} i_{cd} \\ i_{cq} \end{bmatrix} = \begin{bmatrix} -\frac{R_c}{L_c} & \omega \\ -\omega & -\frac{R_c}{L_c} \end{bmatrix} \begin{bmatrix} i_{cd} \\ i_{cq} \end{bmatrix} + \frac{1}{L_c} \begin{bmatrix} D_{nd} \\ D_{nq} \end{bmatrix} v_{\mathrm{dc}} - \frac{1}{L_c} \begin{bmatrix} v_d \\ v_q \end{bmatrix}. \tag{14}$$

As the sum of the three-phase currents is zero, there is no homopolar component ($i_{c0} = 0$); therefore, the ac neutral point voltage does not affect any transformed current. This voltage can be deduced as

$$v_{NM} = \frac{v_0 - v_{0M}}{\sqrt{3}}. \tag{15}$$

It can be seen that the v_{NM} only depends on homopolar voltage components of the converter (v_{0M}) and the grid (v_0). In addition, when the voltage of power grid is balanced, the averaged value of v_0 is zero; therefore, voltage v_{NM} depends only on the homopolar component of the ac voltages of the interfaced converter. Considering the original position of the load voltage vector in d-axis, voltage vector of q-axis will be zero ($v_q = 0$), and the other vector's value will be equal to E_L ($v_d = E_L$), which is the value of the line-to-line rms voltage of grid voltage. Therefore, (14) can be written as

$$\frac{d}{dt} \begin{bmatrix} i_{cd} \\ i_{cq} \end{bmatrix} = \begin{bmatrix} -\frac{R_c}{L_c} & \omega \\ -\omega & -\frac{R_c}{L_c} \end{bmatrix} \begin{bmatrix} i_{cd} \\ i_{cq} \end{bmatrix} + \frac{1}{L_c} \begin{bmatrix} D_{nd} \\ D_{nq} \end{bmatrix} v_{\mathrm{dc}} - \frac{1}{L_c} \begin{bmatrix} E_L \\ 0 \end{bmatrix} \tag{16}$$

where the homopolar component has been omitted.

A. Current Control Technique for Proposed DG Model

In order to obtain a low overshoot, high accuracy, and fast dynamic response to provide load active and reactive power and also harmonic current components of the grid-connected loads, two equations in the equivalent model of the proposed system (14) must be controlled in two different and independent loops. As we mentioned before, all the Park-transformed variables of the DG system will become a constant value in steady-state condition. By this technique, it is possible to design the current controllers using the well-known controller design tools meant for regulation problems instead of having to design more complex controllers to track general time-varying reference signals. By referring to (14) and considering $\lambda = L_c(di_c/dt) + R_c i_c$, switching state functions can be calculated as

$$D_{nd} = \frac{\lambda_d - L_c\omega i_{cq} + v_d}{v_{\rm dc}} \tag{17}$$

$$D_{nq} = \frac{\lambda_q + L_c\omega i_{cd}}{v_{\rm dc}}. \tag{18}$$

As shown in (17) and (18), the crosscoupling terms $L_c\omega i_{cq}$ and $L_c\omega i_{cd}$ exist in circuit of current control loop, and the blocks that contain $L_c\omega$ have the objective of decoupling influenced between both current control loops in the d- and q-axes. Note that the original control inputs D_{nd} and D_{nq} consist of combination of a nonlinearity cancelation part and a linear decoupling compensation part. To achieve a fast dynamic response and zero steady-state errors, particularly during connection of nonlinear loads to the grid, which main grid is polluted by these types of loads, a proportional–integral (PI)-type regulator is needed. The parameter of the proposed regulator can be obtained as

$$(\lambda_{dq}) = k_p(\Delta i_{cdq}) + k_i \int (\Delta i_{cdq})\, dt \tag{19}$$

where terms k_p and k_i are proportional and integral gains, respectively, and $(\Delta i_{cdq}) = (i^*_{cdq}) - (i_{cdq})$ denotes a comparison of the calculated reference currents and the actual DG injection currents generated by the VSC which create error signals and control the switches of the inverter according to objectives of the interconnection of DG system to the grid. The transfer function of the PI regulator for current control loops of proposed strategy is given as

$$G_i(s) = \frac{\lambda_d(s)}{\Delta I_d(s)} = \frac{\lambda_q(s)}{\Delta I_q(s)} = k_p + \frac{k_i}{s}. \tag{20}$$

To design PI regulator in circuit of current controller, it is necessary to decouple the model of the system by adding the measured voltage of d-axis and crosscoupling terms as shown in Fig. 3, where L^* and v^* are estimated values of coupling inductance and grid voltages.

Thus, the inner control loops of the current i_{cd} can be simplified as shown in Fig. 4. As shown in Fig. 3, the current loops of i_{cd} and i_{cq} are the same. Thus, in dq reference frame, decoupled control for the reactive and active power can be conveniently achieved by independently controlling the d- and q-axis currents.

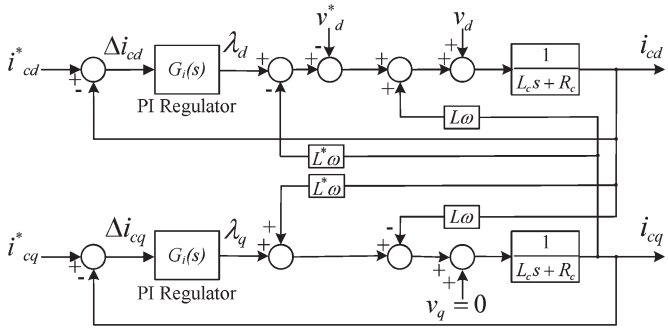

Fig. 3. Inner control loop of the i_{cd} and i_{cq}.

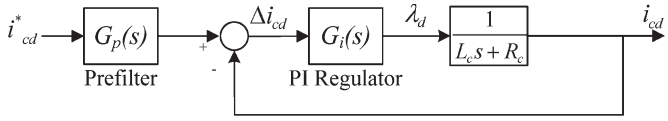

Fig. 4. Equivalent diagram of d-axis current control loop.

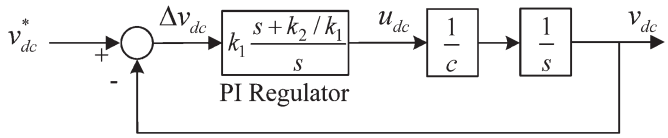

Fig. 5. Control loop of the dc voltage.

The closed-loop transfer function of the current loop can be calculated as

$$\frac{I_{cq}(s)}{I^*_{cq}(s)} = \frac{I_{cd}(s)}{I^*_{cd}(s)} = \frac{k_p}{L_c}\frac{s + \frac{k_i}{k_p}}{s^2 + \frac{(R_c + k_p)}{L_c}s + \frac{k_i}{L_c}}. \tag{21}$$

The transient response of the currents will be affected by the presence of the zero in (21). In particular, the actual percent overshoot will be much higher than expected. For the optimal value of the damping factor $\zeta = \sqrt{1/2}$, the theoretical overshoot is 20.79%. To eliminate the effect of zero on transient response in (21), a prefilter is added as shown in Fig. 4. The response of the current loops becomes that of a second-order transfer function with no zero. Comparison between general model of a second-order transfer function $\omega_n^2/(s^2 + 2\xi\omega_n s + \omega_n^2)$ and (21) leads to the following design relations:

$$k_p = 2L_c\zeta\omega_n - R_c \qquad k_i = L_c \cdot \omega_n^2 \tag{22}$$

where ω_n is natural undamped angular frequency and depends on the specific time response.

VI. DC Voltage Regulation

The error value of the dc-bus voltage $\Delta v_{\rm dc} = v^*_{\rm dc} - v_{\rm dc}$ is passed through a PI-type compensator to regulate the voltage of dc bus $(v_{\rm dc})$ at a fixed value. Therefore, $u_{\rm dc}$ will be obtained as

$$u_{\rm dc} = k_1\Delta v_{\rm dc} + k_2 \int \Delta v_{\rm dc}\, dt \tag{23}$$

where k_1 and k_2 are proportional and integral gains of the proposed PI regulator. Fig. 5 shows the equivalent control circuit loop of the dc-bus voltage for proposed converter.

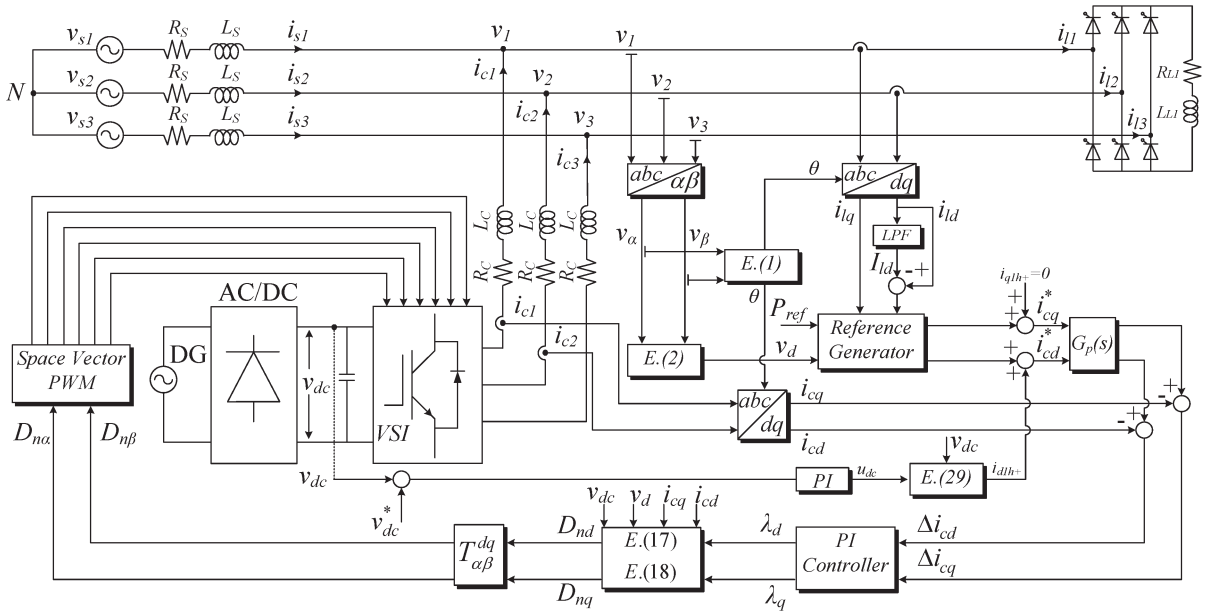

Fig. 6. General schematic diagram of the proposed control strategy for DG system.

The closed-loop transfer function of the proposed dc voltage regulation loop, got from Fig. 5, has the following form:

$$\frac{v_{\rm dc}(s)}{v^*_{\rm dc}(s)} = 2\zeta\omega_{nv}\frac{s+\frac{\omega_{nv}}{2\zeta}}{s^2+2\zeta\omega_{nv}s+\omega^2_{nv}} \tag{24}$$

where the proportional and integral gains are derived from

$$k_1 = 2\zeta\omega_{nv}C \qquad k_2 = \omega^2_{nv}C. \tag{25}$$

The control effort is obtained from

$$i^*_{do} = \frac{u_{\rm dc}-D_{nq}i_q}{D_{nd}} = \frac{u_{\rm dc}v_{\rm dc}-D_{nq}v_{\rm dc}i_q}{D_{nd}v_{\rm dc}}. \tag{26}$$

However, assuming that the current loop is ideal and in normal operation of the active filter, the following properties hold, assuming the supply voltages are given by:

$$\begin{aligned} v_1 &= v\cos(\omega t)\\ v_2 &= v\cos(\omega t-2\pi/3)\\ v_3 &= v\cos(\omega t-4\pi/3). \end{aligned} \tag{27}$$

The transformation to the synchronous reference frame yields

$$\begin{bmatrix} v_d\\ v_q\end{bmatrix} = T^{12}_{dq}\begin{bmatrix} v_1\\ v_2\end{bmatrix} = \sqrt{\frac{3}{2}}\begin{bmatrix} v\\ 0\end{bmatrix}. \tag{28}$$

As a result, $D_{nq}v_{\rm dc}\approx v_q=0$ and $D_{nd}v_{\rm dc}\approx v_d=\sqrt{(3/2)}v$.

Hence, the control effort can be approximated by

$$i_{d1h+}\approx\sqrt{\frac{2}{3}}\cdot\frac{v_{\rm dc}}{v}u_{\rm dc}. \tag{29}$$

The reference current in (29) is added to the harmonic reference current of the loop of i_{ld}. i_{d1h+} is a dc component, and it will force the active filter to generate or to draw a current at the fundamental frequency. Furthermore, by designing the dc voltage loop much slower than the current loop, there would not be any interaction between the two loops.

VII. Simulation Analysis and Results

In order to demonstrate the high performance of the proposed control technique, the complete system model was simulated using the "Power System Blockset" simulator operating under the Matlab/Simulink environment. The schematic diagram and principle of the proposed model and the control technique in an ac grid are shown in Fig. 6. The test model contains a power converter with power rating of 20 kVA. The maximum available value of DG source active power is 8 kW, which is also the active power reference included in the simulations. At first, capabilities of DG resources and flexibility of proposed control strategy to control the proposed VSC in providing active, reactive, and harmonic current components of different loads are shown, and the capabilities of proposed control method on reactive power tracking with constant output active power are considered. In addition, the simulated results have been used to analyze the total harmonic distortion (THD) of the utility grid current amid severe varying load conditions. During the simulation process, constant dc voltage sources have been considered as a DG source. In addition, the active power which is delivered from the DG link to the ac grid is considered to be constant. This assumption makes it possible to evaluate the capability of the proposed control strategy to track the fast change in the active and reactive power, independent of each other. For this purpose, when one of them is changed, another one must be constant. To simulate a real ac grid, the load is connected and disconnected to the power grid randomly, and grid current waveform will be compared with each other under various loads and conditions.

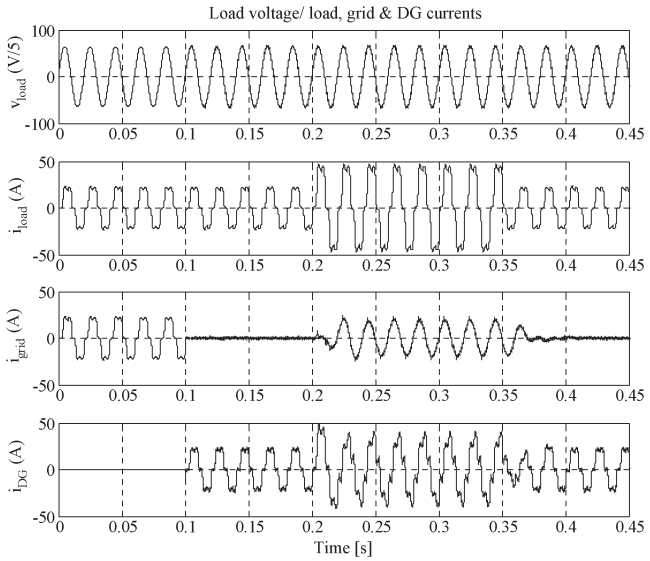

Fig. 7. Load voltage, load, grid, and DG currents before and after connection of DG and before and after connection and disconnection of additional load into the grid.

A. Connection of DG Link to the Grid to Supply Harmonic Current Components and Nonlinear Load Increment

Prior to the connection of DG link to the grid, a full-wave thyristor converter supplies a load with resistance of 20 Ω and 10-mH inductors in each phase. This nonlinear load draws harmonic currents from the grid continuously. The DG link is connected to the ac grid at $t = 0.1$ s. This process is continued until $t = 0.2$; at this moment, another full-wave thyristor converter similar to the prior load is connected to the grid, and it is disconnected from the grid at $t = 0.35$ s. Fig. 7 shows the load voltage (v_l), load current (i_l), grid current $(i_{\rm grid})$, and DG current $(i_{\rm DG})$ in phase (a). As shown in this figure, after the connection of DG link to the grid at $t = 0.1$ s, the grid current becomes zero, and all the active and reactive current components including fundamental and harmonic frequencies are provided by DG link $(i_{\rm grid} = i_{\rm load} - i_{\rm DG})$. In this case, load current is completely equal to reference current of converter; therefore, VSC injects the maximum available power of DG source to the power grid. As a result, the injected current from the grid will be zero. The load current is fed from nonlinear link continuously until the connection of additional load to the grid.

Fig. 8(a) shows that, after connection of additional load to the power grid at $t = 0.2$ s, converter injects the maximum active and reactive power by connection of DG source to the grid. However, in this case, the maximum power of proposed converter is less than the power which is needed to supply the grid-connected loads. Therefore, the remaining power is injected by the utility grid. As shown in this figure, the utility grid injects high-power quality current waveforms even under the connection of nonlinear loads to the grid, and load harmonic currents are provided by DG. There are some sharp edges on current waveforms which are related to high-order harmonic frequencies and created during switching of thyristor converters. In addition, the production in control circuit of DG system is delayed for around one cycle. This is due to the settling time of proposed MPHPF filter, in DG's control loop. Fig. 8(b)

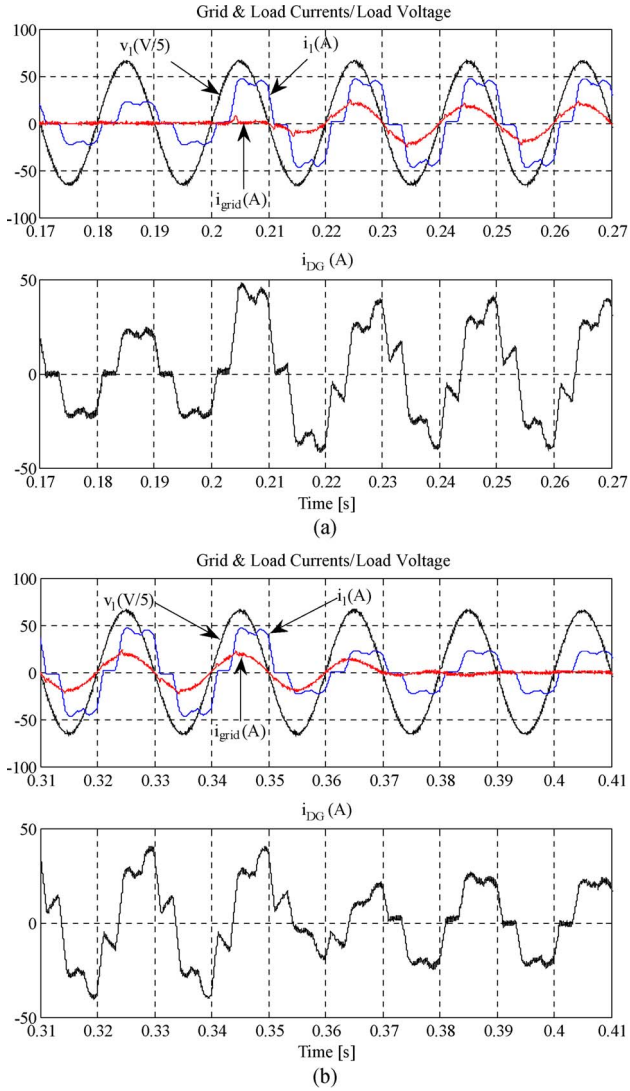

Fig. 8. Grid, load, DG currents, and load voltage (a) before and after connection of additional load and (b) before and after disconnection of additional load.

shows that, with the same delay as before, additional load is removed at $t = 0.35$ s. As shown in this figure, after the pass of the transient times, the injected current from grid to the load becomes zero, and DG link supplies all the required power to supply the proposed nonlinear load.

Fig. 9 shows that, after the transient times during connection of additional load to the main grid, the load voltage and grid current are in phase, and the grid does not need to provide reactive and harmonic currents for the load which is shown for three phases.

The ability of control loop to track the reference current trajectories of d- and q-axes, during connection of DG link to the grid and, also, connection of additional load to the grid, is shown in Fig. 10. Fig. 10(a) shows that, before connection of additional load to the grid, the actual d- and q-axis current components of DG's control loop track their reference trajectory precisely. However, according to Fig. 10(b), after connection of additional load to the grid, the actual d-axis current component of DG tracks half of its reference trajectory which is equal to

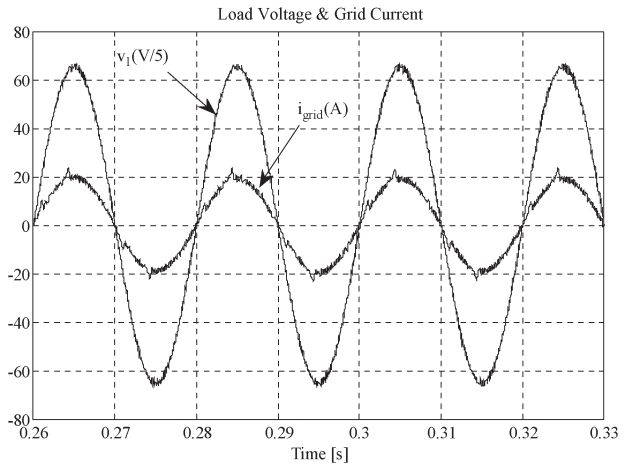

Fig. 9. Phase-to-neutral voltage and grid current for phase (a).

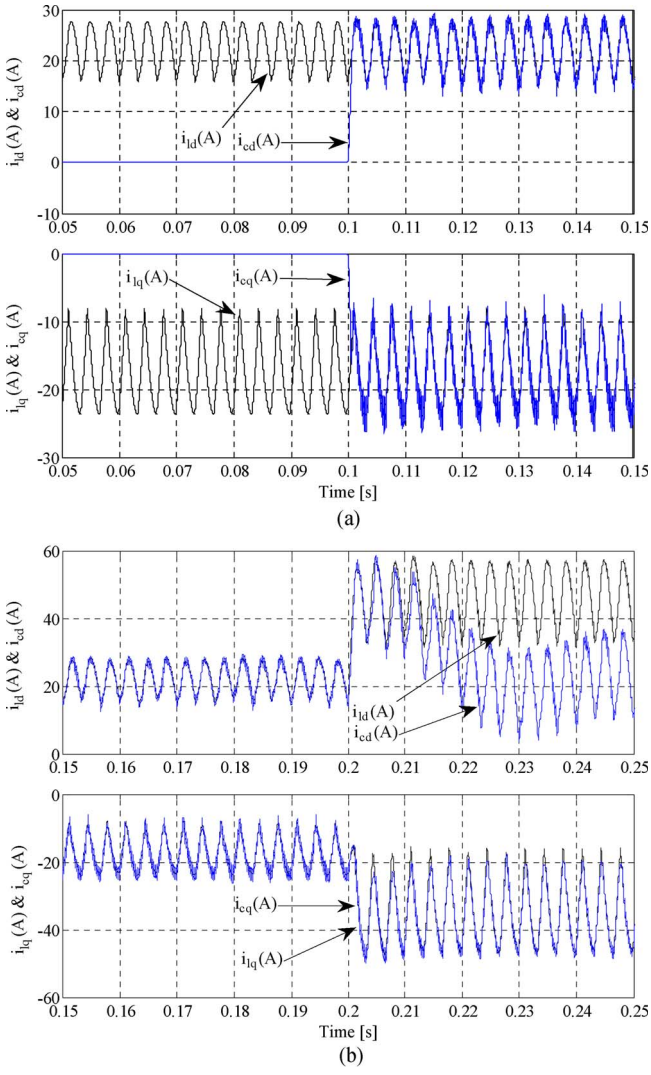

Fig. 10. Reference currents track the load current (a) after interconnection of DG resources and (b) after additional load increment.

its maximum active power (reference active power), and all the reference trajectories of reactive current change.

Spectrum analysis results of load and grid currents depicted in Table I indicate that the DG link can largely improve the

TABLE I
FUNDAMENTAL AND THD VALUES OF GRID CURRENTS

Before Compensation				After Compensation		
Peak Current (A)	I_{grid1}	I_{grid2}	I_{grid3}	I_{grid1}	I_{grid2}	I_{grid3}
Fundamental	47.16	47.23	47.64	17.67	17.73	17.54
THD%	21.39	21.29	21.84	4.26	4.28	4.35

THD of the grid currents while feeding nonlinear loads. The THDs of the grid currents are reduced from 21.39%, 21.29%, and 21.84% before compensation to 4.26%, 4.28%, and 4.35% after compensation, respectively. These results confirm the capability of the proposed DG link to compensate harmonic currents of the nonlinear loads.

The trajectories of the load, grid, and DG currents in $\alpha\beta$ representation are shown in Fig. 11. Fig. 11(a) shows the trajectory of the load currents in $\alpha\beta$ representation, which is required to supply the load, before and after connection of additional load to the PCC. It can be seen that the ac currents are containing some harmonic current distortion for feedforward modulation, so the $\alpha\beta$ representation of those currents is not circular and is hexagonal. In addition, after the second load similar to first load is connected to the ac grid, radius of external hexagonal is exactly two times greater than radius of internal hexagonal. Fig. 11(b) and (c) shows the trajectory of the grid and DG currents in $\alpha\beta$ representation, before and after connection of additional load to the grid. As it can be seen in Fig. 11(b), after connection of additional load to the PCC, the grid current does not contain significant low-frequency distortion for feedforward modulation, since the $\alpha\beta$ representation of those currents is approximately circular. Fig. 11(c) shows that, after connection of second load to the grid, DG link supplies the harmonic current components of d- and q-axes and half of active power and whole of the reactive power of the grid-connected loads.

B. Connection of DG Link to an Unbalanced Grid

In this section, the ability of proposed DG link to track load current components for unbalanced grid voltage is evaluated. At first, a nonlinear load similar to the prior load is added to the PCC at $t = 0.45$ s. At $t = 0.55$ s, the grid voltage is unbalanced. Fig. 12 shows three-phase grid voltages, load current, grid current, and DG link current. As shown in Fig. 12, load harmonic current components are provided by DG link, and grid currents are maintained sinusoidal during balanced and unbalanced grid voltages. In addition, load voltage and grid current are kept in phase (the grid does not provide reactive current). The proposed control scheme provides balanced current injection from the DG link. Therefore, since the grid voltage unbalance forces unbalanced current in the load, the grid current is unbalanced. Depending on the power converter current ratings and voltage unbalance severity, it could be possible to compensate the grid currents unbalance by injecting unbalance currents from the DG link [32], but this is not the purpose of the present control scheme.

VIII. HARDWARE IMPLEMENTATION AND TEST RESULTS

The general schematic diagram of the experimental setup is shown in Fig. 13, where the positive polarities for grid current

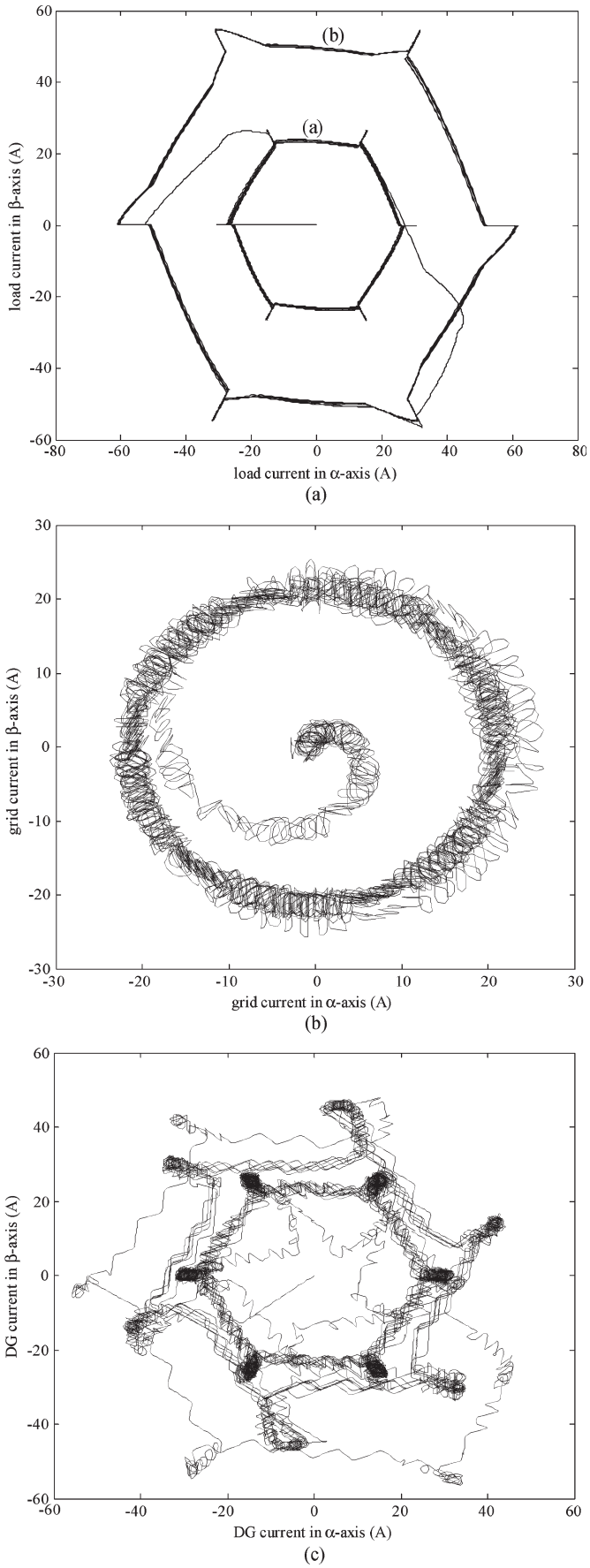

Fig. 11. Trajectories of the (a) load, (b) grid, and (c) DG currents before and after connection of additional load to the grid in $\alpha\beta$ representation.

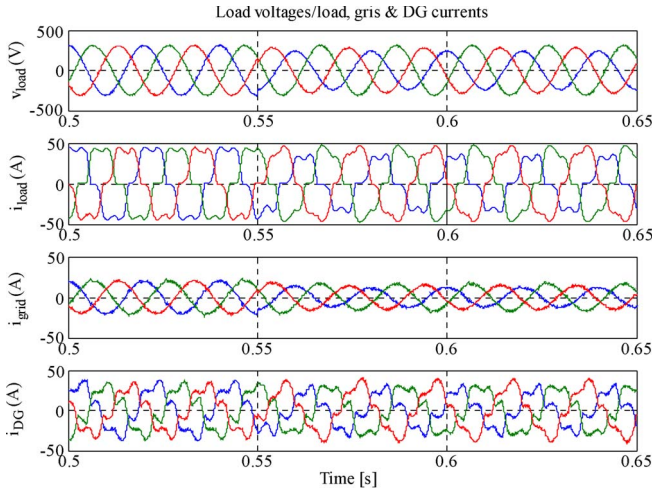

Fig. 12. Load voltage, load, grid, and DG currents during connection of DG link to the unbalanced grid voltage.

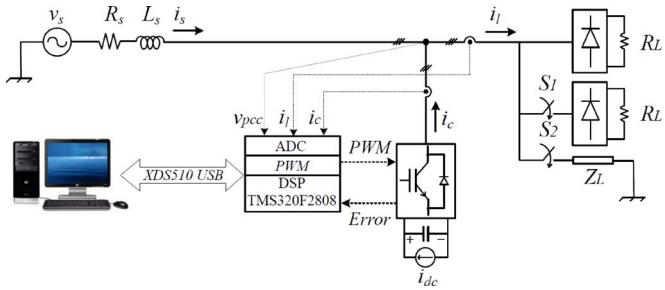

Fig. 13. Experimental setup of the proposed DG model.

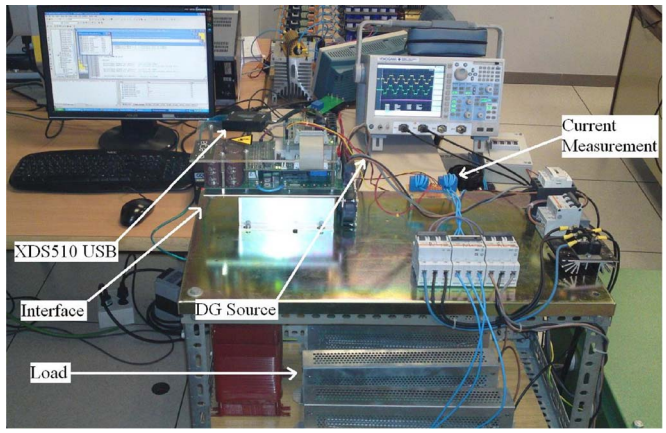

Fig. 14. General view of the experimental test bench.

(i_s), load current (i_l), and DG current (i_c) are emphasized, in agreement with Fig. 6. A general view of the experimental test bench is shown in Fig. 14, and the system parameters are given in Table II. A 2-kVA three-phase full-bridge converter prototype using a switching frequency of 10 kHz has been used for the experimental tests. The hardware platform used to implement the converter control algorithm is TMS320F2808 digital signal processor. The quantities measured from the proposed system are the converter current (i_c), the PCC voltage $(v_{\rm pcc})$, and the grid-connected load current (i_l), as shown in Fig. 13. As this paper's focus is on the grid-connected converter,

TABLE II
EXPERIMENTAL SETUP PARAMETERS

Parameter	Value
Grid voltage	230 V
Interfacing inductance	4.6 mH
DC-link capacitance	1020 μF
DC-link voltage setpoint	610 V
Switching/Sampling frequency	10 kHz
Fundamental frequency	50 Hz
Linear load resistance	40 Ω
Linear load inductance	100 mH
Nonlinear load resistance	180 Ω

the dc energy source has been emulated with a three-phase diode rectifier fed by a three-phase alternative voltage source.

The available DG source power is 320 W, which is also the active power reference included in the real-time tests. The main purposes of the experimental tests are to study different performance aspects in different conditions. At first, the capabilities of DG source and flexibility of the proposed control strategy for control of VSC in providing active, reactive, and harmonic current components of grid-connected loads are shown, and the capabilities of proposed control method on reactive power tracking with constant output active power are considered. In addition, the active power which is delivered from the DG sources to the grid is considered to be constant. This assumption makes it possible to evaluate the capability of the proposed control strategy to track the fast change in the active and reactive power, independent of each other. For this purpose, when one of them is changed, another one must be constant. To consider a real power grid, the loads are connected and disconnected to power grid randomly, and grid current waveform will be compared with each other under various load connection and conditions.

A. *Ability of Proposed Strategy to Supply Grid-Connected Loads*

This test has been performed with the converter having only nonlinear local load which is connected to the utility grid. Prior to the connection of DG link to the ac grid, a three-phase full-wave diode rectifier supplies a resistive load with a resistance of 30 Ω in each phase. This nonlinear load draws harmonic current from the grid continuously and makes harmonic pollutants in utility grid.

Fig. 15 shows the load, grid, and DG currents before and after connection of DG link to the grid. As shown in this figure, before connection of DG link to the grid, all the nonlinear current components are injected by main grid to the nonlinear load. This process is continued until the DG link is connected to the main grid. After connection of DG link to the grid, the grid current becomes zero, and all the active and reactive current components including fundamental and harmonic frequencies are provided by DG link ($i_{\rm grid} = i_{\rm load} - i_{\rm DG}$). It can be seen that the problems due to synchronization between DG and power grid do not exist and DG link can be connected to the proposed grid without any high-current overshoot.

The proposed load's current is fed from nonlinear DG link continuously, and this process is continued until another full-wave diode rectifier similar to the prior load is connected to the grid. Fig. 16 shows the transient waveforms of the dc-bus voltage, load, grid, and DG currents before and after sudden variation in the current-source type of nonlinear load. It can be seen that, after connection of additional load to the grid, production in control circuit of DG system is delayed for less than half a cycle. This is due to settling time of MPHPF filter in control loop of DG system. In addition, load harmonic currents are provided by DG, and grid current is sinusoidal; however, there are sharp edges on grid current waveforms which are related to high-order harmonic frequencies and created during switching of thyristor converters. In addition, Fig. 16 shows that the dc-bus voltage of the VSC is well regulated and no overvoltage appears in the transient state. Therefore, proposed integration strategy is insensitive to grid overload during connection of DG resources to the power grid.

Fig. 17 shows that, after connection of additional load to the power grid, the load voltage and grid current are in phase, so the

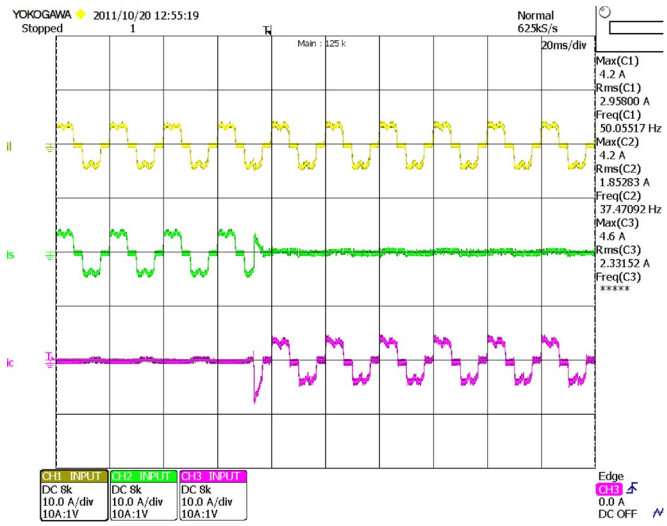

Fig. 15. Load, grid, and DG currents before and after connection of DG link to the power grid.

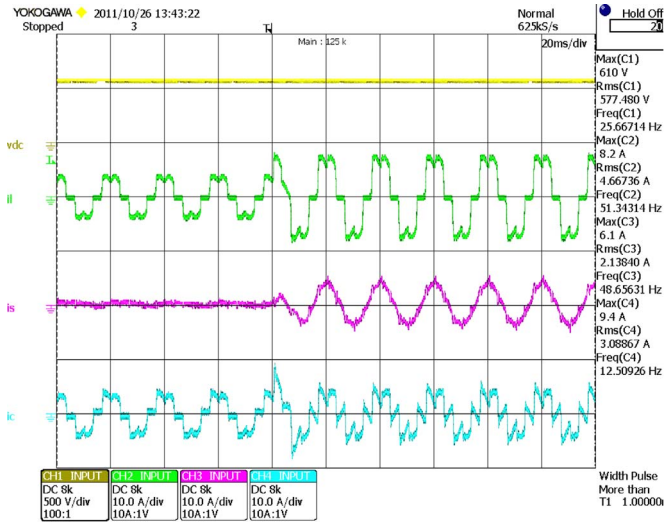

Fig. 16. DC-bus voltage, load, grid, and DG currents before and after connection of additional load to the grid.

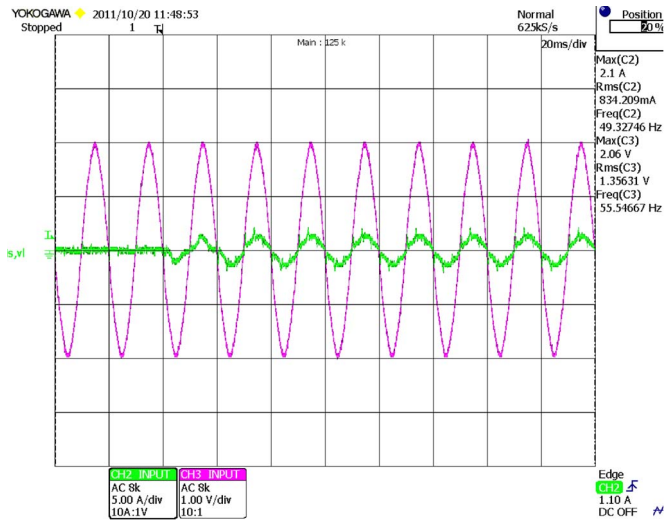

Fig. 17. Phase-to-phase voltage and grid current for phases (ab).

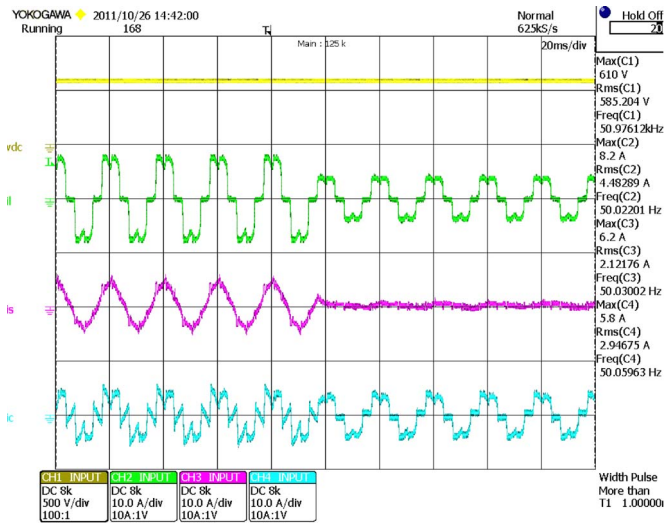

Fig. 18. DC-bus voltage, load, grid, and DG currents before and after the removal of additional load from the grid.

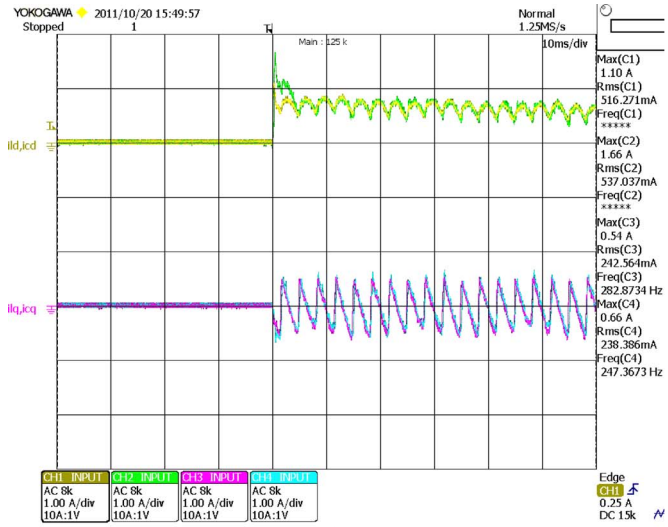

(a)

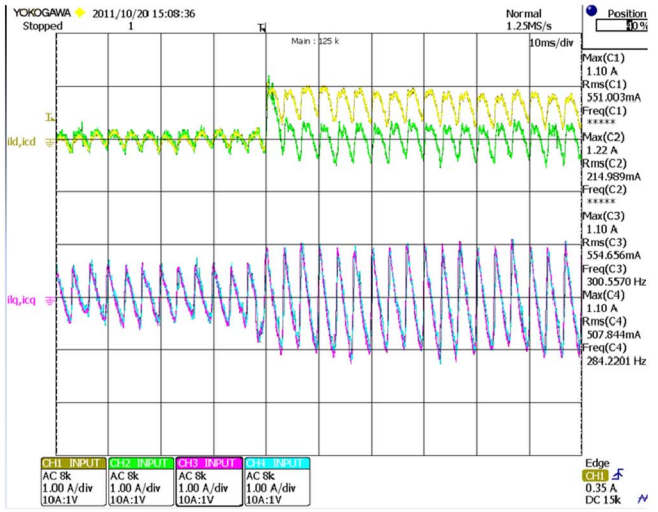

(b)

Fig. 19. Reference currents track the load current (a) after integration of DG and (b) after additional load increment.

grid does not need to provide reactive and harmonic currents for the grid-connected loads. In this case, the local loads still draw active power from the main grid. This happens because the maximum reference active power of proposed converter is less than the active power requested by the local loads.

Fig. 18 shows that, with the same delay as before, additional load is removed and, after the pass of the transient times, the grid current becomes zero; therefore, all the active and reactive current components of the proposed nonlinear load including fundamental and harmonic frequencies are provided by the DG link.

The ability of the proposed control loop to track the reference current of d- and q-axes, for the duration of connection of DG link and for the period of connection of additional load to the grid, is shown in Fig. 19. As shown in Fig. 19(a), before connection of additional load to the main grid, DG link fallows both active and reactive reference currents completely. However, according to Fig. 19(b), after connection of additional load to the main grid, DG fallows half of the reference active current in fundamental frequency, whole of the reference reactive current, and whole of the active and reactive currents in fundamental frequencies. The remaining active current in fundamental frequency is injected by the grid.

Fig. 20 shows the steady-state operations of the DG link for injection of maximum available power from DG source to the power grid when the grid-connected loads are disconnected. As shown in this figure, the grid current is out of phase with respect to the converter current by 180 electrical degrees, which means maximum active power injected from DG to the grid continuously.

IX. Conclusion

A multiobjective control algorithm for the grid-connected converter-based DG interface has been proposed and presented in this paper. Flexibility of the proposed DG in both steady-state and transient operations has been verified through simulation and experimental results.

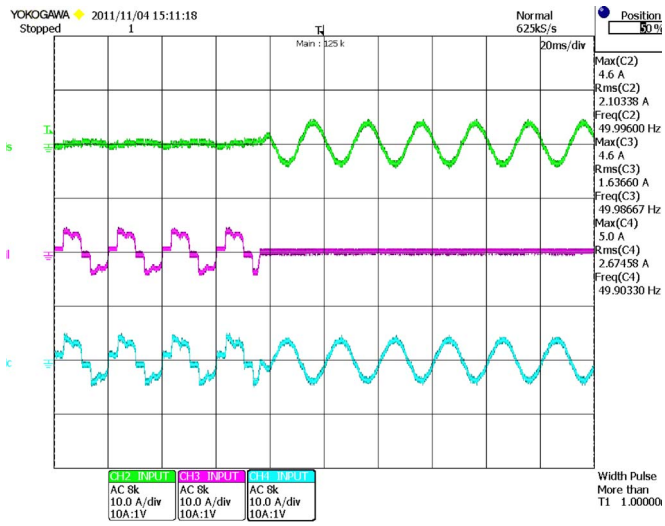

Fig. 20. Steady-state operation of the proposed DG link for injection of maximum available active power to the power grid continuously.

Due to sensitivity of phase-locked loop to noises and distortion, its elimination can bring benefits for robust control against distortions in DG applications. Also, the problems due to synchronization between DG and grid do not exist, and DG link can be connected to the power grid without any current overshoot. One other advantage of proposed control method is its fast dynamic response in tracking reactive power variations; the control loops of active and reactive power are considered independent. By the use of the proposed control method, DG system is introduced as a new alternative for distributed static compensator in distribution network. The results illustrate that, in all conditions, the load voltage and source current are in phase and so, by improvement of power factor at PCC, DG systems can act as power factor corrector devices. The results indicate that proposed DG system can provide required harmonic load currents in all situations. Thus, by reducing THD of source current, it can act as an active filter. The proposed control technique can be used for different types of DG resources as power quality improvement devices in a customer power distribution network.

REFERENCES

[1] T. Zhou and B. François, "Energy management and power control of a hybrid active wind generator for distributed power generation and grid integration," *IEEE Trans. Ind. Electron.*, vol. 58, no. 1, pp. 95–104, Jan. 2011.

[2] M. Singh, V. Khadkikar, A. Chandra, and R. K. Varma, "Grid interconnection of renewable energy sources at the distribution level with power-quality improvement features," *IEEE Trans. Power Del.*, vol. 26, no. 1, pp. 307–315, Jan. 2011.

[3] M. F. Akorede, H. Hizam, and E. Pouresmaeil, "Distributed energy resources and benefits to the environment," *Renewable Sustainable Energy Rev.*, vol. 14, no. 2, pp. 724–734, Feb. 2010.

[4] C. Mozina, "Impact of green power distributed generation," *IEEE Ind. Appl. Mag.*, vol. 16, no. 4, pp. 55–62, Jun. 2010.

[5] B. Ramachandran, S. K. Srivastava, C. S. Edrington, and D. A. Cartes, "An intelligent auction scheme for smart grid market using a hybrid immune algorithm," *IEEE Trans. Ind. Electron.*, vol. 58, no. 10, pp. 4603–4611, Oct. 2011.

[6] W. El-Khattam and M. M. A. Salama, "Distributed generation technologies, definitions and benefit," *Elect. Power Syst. Res.*, vol. 71, no. 2, pp. 119–128, Oct. 2004.

[7] E. Pouresmaeil, D. Montesinos-Miracle, O. Gomis-Bellmunt, and J. Bergas-Jané, "A multi-objective control strategy for grid connection of DG (distributed generation) resources," *Energy*, vol. 35, no. 12, pp. 5022–5030, Dec. 2010.

[8] F. Blaabjerg, R. Teodorescu, M. Liserre, and A. V. Timbus, "Overview of control and grid synchronization for distributed power generation systems," *IEEE Trans. Power Electron.*, vol. 53, no. 5, pp. 1398–1409, Oct. 2006.

[9] F. Blaabjerg, Z. Chen, and S. Kjaer, "Power electronics as efficient interface in dispersed power generation systems," *IEEE Trans. Power Electron.*, vol. 19, no. 5, pp. 1184–1194, Sep. 2004.

[10] G. Saccomando and J. Svensson, "Transient operation of grid-connected voltage source converter under unbalanced voltage conditions," in *Proc. IAS*, Chicago, IL, Oct. 2001, vol. 4, pp. 2419–2424.

[11] R. Teodorescu and F. Blaabjerg, "Flexible control of small wind turbines with grid failure detection operating in stand-alone or grid-connected mode," *IEEE Trans. Power Electron.*, vol. 19, no. 5, pp. 1323–1332, Sep. 2004.

[12] M. Kazmierkowski, R. Krishnan, and F. Blaabjerg, *Control in Power Electronics—Selected Problems*. New York: Academic, 2002.

[13] E. Twining and D. G. Holmes, "Grid current regulation of a three-phase voltage source inverter with an *LCL* input filter," *IEEE Trans. Power Electron.*, vol. 18, no. 3, pp. 888–895, May 2003.

[14] M. K. Ghartemani and M. Iravani, "A method for synchronization of power electronic converters in polluted and variable-frequency environments," *IEEE Trans. Power Syst.*, vol. 19, no. 3, pp. 1263–1270, Aug. 2004.

[15] U. Borup, F. Blaabjerg, and P. N. Enjeti, "Sharing of nonlinear load in parallel-connected three-phase converters," *IEEE Trans. Ind. Appl.*, vol. 37, no. 6, pp. 1817–1823, Nov./Dec. 2001.

[16] Y. A.-R. I. Mohamed, "Mitigation of grid-converter resonance, grid-induced distortion and parametric instabilities in converter-based distributed generation," *IEEE Trans. Power Electron.*, vol. 26, no. 3, pp. 983–996, Mar. 2011.

[17] H. Karimi, A. Yazdani, and R. Iravani, "Robust control of an autonomous four-wire electronically-coupled distributed generation unit," *IEEE Trans. Power Del.*, vol. 26, no. 1, pp. 455–466, Jan. 2011.

[18] V. Calderaro, V. Galdi, and A. Picolo, "Distribution planning by genetic algorithm with renewable energy units," in *Proc. Bulk Power Syst. Dyn. Control*, Cortina d'Ampezzo, Italy, 2004, vol. 1, pp. 375–380.

[19] M. Kim, R. Hara, and H. Kita, "Design of the optimal ULTC parameters in distribution system with distributed generations," *IEEE Trans. Power Syst.*, vol. 24, no. 1, pp. 297–305, Feb. 2009.

[20] J.-H. Teng, C.-Y. Chen, C.-F. Chen, and Y.-H. Liu, "Optimal capacitor control for unbalanced distribution systems with distributed generations," in *Proc. IEEE ICSET*, Singapore, 2008, pp. 755–760.

[21] H. Hatta, S. Uemura, and H. Kobayashi, "Demonstrative study of control system for distribution system with distributed generation," in *Proc. IEEE/PES Power Syst. Conf. Expo.*, Seattle, WA, 2009, pp. 1–6.

[22] M. E. Baran and F. F. Wu, "Network reconfiguration in distribution systems for loss reduction and load balancing," *IEEE Trans. Power Del.*, vol. 4, no. 2, pp. 1401–1407, Apr. 1989.

[23] C. C. Liu, S. J. Lee, and K. Vu, "Loss minimization for distribution feeders: Optimality and algorithms," *IEEE Trans. Power Del.*, vol. 4, no. 2, pp. 1281–1289, Apr. 1989.

[24] J. Olamaei, T. Niknam, and G. Gharehpetian, "Impact of distributed generators on distribution feeder reconfiguration," in *Proc. IEEE Lausanne Power Tech*, Lausanne, Switzerland, 2007, pp. 1747–1751.

[25] S. Yang, Q. Lei, F. Z. Peng, and Z. Qian, "A robust control scheme for grid-connected voltage-source inverter," *IEEE Trans. Ind. Electron.*, vol. 58, no. 1, pp. 202–212, Jan. 2011.

[26] J. He, Y. W. Li, and M. S. Munir, "A flexible harmonic control approach through voltage-controlled DG-grid interfacing converters," *IEEE Trans. Ind. Electron.*, vol. 59, no. 1, pp. 444–455, Jan. 2012.

[27] I.-Y. Chung, W. Liu, D. A. Cartes, E. G. Collins, and S. Moon, "Control methods of inverter-interfaced distributed generators in a microgrid system," *IEEE Trans. Ind. Electron.*, vol. 46, no. 3, pp. 1078–1088, May/Jun. 2010.

[28] C. A. Busada, S. G. Jorge, A. E. Leon, and J. A. Solsona, "Current controller based on reduced order generalized integrators for distributed generation systems," *IEEE Trans. Ind. Electron.*, vol. 59, no. 7, pp. 2898–2909, Jul. 2012.

[29] I. J. Balaguer, Q. Lei, S. Yang, U. Supatti, and F. Z. Peng, "Control for grid-connected and intentional islanding operations of distributed power generation," *IEEE Trans. Ind. Electron.*, vol. 58, no. 1, pp. 147–157, Jan. 2011.

[30] S. Alepuz, S. Busquets-Monge, J. Bordonau, J. Gago, D. González, and J. Balcells, "Interfacing renewable energy sources to the utility grid using a three-level inverter," *IEEE Trans. Ind. Electron.*, vol. 53, no. 5, pp. 1504–1511, Oct. 2006.
[31] S. Rahmani, N. Mendalek, and K. Al-Haddad, "Experimental design of a nonlinear control technique for three-phase shunt active power filter," *IEEE Trans. Ind. Electron.*, vol. 57, no. 10, pp. 3364–3375, Oct. 2010.
[32] A. Junyent-Ferré, O. Gomis-Bellmunt, T. C. Green, and D. E. Soto-Sanchez, "Current control reference calculation issues for the operation of renewable source grid interface VSCs under unbalanced voltage sags," *IEEE Trans. Power Electron.*, vol. 26, no. 12, pp. 3744–3753, Dec. 2011.

Edris Pouresmaeil was born in Babol, Iran, in 1979. He received the B.Sc. and M.Sc. degrees in electrical engineering from the University of Mazandaran, Babol, in 2003 and 2005, respectively, and the Ph.D. degree in electrical engineering from the Technical University of Catalonia (UPC), Barcelona, Spain, in 2012.

He is currently a Postdoctoral Fellow with the Department of Electrical and Computer Engineering, University of Waterloo, Waterloo, ON, Canada. His research interests include distributed generation (DG), operation and control strategies, digital signal processor control applications for high-power and DG systems, and modeling and control of multilevel converters for integration of renewable energy resources to the power grid, microgrid, and smart grid operations.

Carlos Miguel-Espinar was born in Barcelona, Spain, on November 6, 1985. He received the M.Sc. degree in industrial engineering from the Escola Tècnica Superior d'Enginyers Industrials de Barcelona-Universitat Politècnica de Catalunya, Barcelona, in 2011, where he started his Master's thesis about the design and implementation of a power photovoltaic (PV) emulator for testing PV inverters in the research center "Centre d'Innovació Tecnològica en Convertidors Estàtics i Accionaments (CITCEA)" in 2010.

He is currently with CITCEA-UPC, as a Project Engineer developing tasks focused on the design of electrical motor for washing machine and advanced control of multilevel converter for integration of distributed energy resources into the grid.

Miquel Massot-Campos was born in Mallorca on September 21, 1988. He received the M.Sc. degree in industrial engineering from the School of Industrial Engineering of Barcelona (ETSEIB), Technical University of Catalonia (UPC), Barcelona, Spain, in 2011.

From 2009 to May 2012, he was with the Centre d'Innovació Tecnològica en Convertidors Estàtics i Accionaments (CITCEA) research group, Department of Electrical Engineering, UPC. Since April 2012, he has been with the SRV-UIB, Palma de Mallorca, Spain. His research interests include the fields linked with power electronics, renewable energy integration in power systems, industrial automation, computer vision, and robotics.

Daniel Montesinos-Miracle (S'01–M'08) was born in Barcelona, Spain, in 1975. He received the M.Sc. degree in electrical engineering from the School of Industrial Engineering of Barcelona (ETSEIB), Technical University of Catalonia (UPC), Barcelona, Spain, in 2000 and the Ph.D. degree from the UPC in 2008.

In 2001, he was with Salicru Electronics, S.A., Santa Maria de Palautordera, Spain, as a Research and Development Engineer. Since 2001, he has been a Research Collaborator with the Centre d'Innovació Tecnològica en Convertidors Estàtics i Accionaments (CITCEA), Department of Electrical Engineering, UPC, where he became a Lecturer with the Department of Electrical Engineering in 2005. His primary research interests are power electronics, drives, and green energy converters.

Oriol Gomis-Bellmunt (S'05–A'07–M'07–SM'12) received the degree in industrial engineering from the School of Industrial Engineering of Barcelona (ETSEIB), Technical University of Catalonia (UPC), Barcelona, Spain, in 2001, and the Ph.D. degree in electrical engineering from the UPC in 2007. In 2003, he developed part of his Ph.D. thesis in the German Aerospace Center (DLR), Braunschweig, Germany.

In 1999, he was with Engitrol S.L. as a Project Engineer in the Automation and Control Industry. Since 2004, he has been with the Department of Electrical Engineering, UPC, where he is a Lecturer and participates in the Centre d'Innovació Tecnològica en Convertidors Estàtics i Accionaments (CITCEA) research group. Since 2009, he has also been with the Catalonia Institute for Energy Research (IREC), Barcelona. His research interests include the fields linked with smart actuators, electrical machines, power electronics, renewable energy integration in power systems, industrial automation, and engineering education.